DATA RESOLUTION MATRIX OF HIGH-FREQUENCY RAYLEIGH-WAVE PHASE VELOCITIES

Jianghai Xia, Kansas Geological Survey, The University of Kansas, Lawrence, Kansas
Richard D. Miller, Kansas Geological Survey, The University of Kansas, Lawrence, Kansas
Yixian Xu, Open Laboratory of Engineering Geophysics of China Department of Land and Resources, China University of Geosciences, Wuhan, China

Abstract

High-frequency (≥ 2 Hz) Rayleigh-wave phase velocities have been utilized to determine shear (S)-wave velocities in near-surface geophysics since the early 1980s. For a given near-surface geophysical problem, it is essential to understand how well the data, calculated according to a layered earth model, might match the observed data. It is also important to recognize that the match may only be possible for data in a certain frequency range because the sensitivity of Rayleigh-wave phase velocities due to changes in S-wave velocities varies with frequency. The data resolution matrix is not a function of the data, but only of the data kernel (the Jacobian matrix, determined by a geophysical model and a priori information applied to the problem). The data resolution matrix of high-frequency Rayleigh-wave phase velocities, therefore, offers a quantitative tool for design of field surveys and prediction of the match between calculated and observed data. We employ the data resolution matrix to discuss the resolving power of phase velocities at different frequencies and the advantages of higher modes. Our discussion provides insights into the inversion of Rayleigh-wave phase velocities. Because of restrictions of the data kernel of the inversion system, each near-surface geophysical problem can be resolved only with Rayleigh-wave phase velocities in a specific frequency range and higher modes normally possess higher resolving power than the fundamental mode.

Introduction

Elastic properties of near-surface materials and their effects on seismic wave propagation are of fundamental interest in ground-water, engineering, and environmental studies. Shear (S)-wave velocities can be derived from inverting dispersive phase velocities of the surface waves (Rayleigh and/or Love) (e.g., Dorman and Ewing, 1962; Aki and Richards, 1980, p. 664). Spectral Analysis of Surface Waves (SASW) (Stokoe and Nazarian, 1983; Stokoe et al., 1989) analyzes the dispersion curve of ground roll to produce near-surface S-wave velocity profiles. The other method proposed by Song et al. (1989) utilizes a multichannel recording system to estimate near-surface S-wave velocities from high-frequency surface waves. Park et al. (1999) study the near-offset and far-offset effects of multichannel analysis of surface waves (MASW). Xia et al. (1999) analyze parameter sensitivity of high-frequency (≥ 2 Hz) Rayleigh waves and presented a stable inversion algorithm. The MASW method possesses the advantage of easily recognizing surface waves, effectively eliminating body-wave energy, and accurately defining dispersion energy. Errors associated with S-wave velocities obtained by the MASW method are 15% or less and random after comparison with direct borehole measurements (Xia et al., 2000a and 2002a). If higher mode data are available, the accuracy of the inverted S-wave velocity can

be significantly improved (Xia et al., 2000b, 2003; Beaty et al., 2002; Beaty and Schmitt, 2003). Xia et al. (2003) indicated at least two quite exciting higher mode properties by analysis of the Jacobian matrix. First, for fundamental and higher mode Rayleigh wave data with the same wavelength, higher modes can "see" deeper than the fundamental mode. Second, higher mode data can increase resolution of inverted S-wave velocities. More authors have studied advantages of using higher modes in estimation of S-wave velocities (e. g., Song et al., in press; Luo, et al., in review; Liang and Chen, in review). Their work demonstrates that S-wave velocities can be accurately determined with synthetic and real data if higher modes are available and inverted.

In this paper, we demonstrate that the data resolution matrix reveals property of higher modes in inversion. First, we provide the background of the data resolution matrix. Second, we use synthetic and real data examples to show that higher mode data can generally be resolved more easily than the fundamental mode data. Finally, we demonstrate with these data that only resolvable data are needed to obtain accurate S-wave velocities in Rayleigh-wave data inversion. In practice, the data resolution matrix can indicate that certain phase velocities are necessary to define the S-wave velocity for a given geological problem. In other words, if these data (phase velocities in a certain frequency range or at certain frequencies) are not available, the given geological problem (S-wave velocity model) cannot be solved.

Data Resolution Matrix

Near-surface S-wave velocities can be estimated by inverting phase velocities of high-frequency Rayleigh waves (Xia et al., 1999, 2003, and 2006). Near-surface quality factors (Q), which is directly related to the material damping ratio D (Q^{-1} = 2D) (Rix et al., 2000), can also be determined by inverting attenuation coefficients of Rayleigh waves (Xia et al., 2002b). Both techniques are based on the overdetermined system

$$\mathbf{G}\mathbf{m}^{\text{true}} = \mathbf{d}, \tag{1}$$

where $\mathbf{G}$ is an m $\times$ n matrix (m > n in both cases), and $\mathbf{m}^{\text{true}}$ and $\mathbf{d}$ are model and data vectors, respectively. $\mathbf{G}$ stands for a data kernel that embodies $\mathbf{m}^{\text{true}}$ and experimental geometry. Letting $\mathbf{H}$ be a generalized inverse of $\mathbf{G}$, we get an estimated model $\mathbf{m}^{\text{est}}$

$$\mathbf{m}^{\text{est}} = \mathbf{H}\mathbf{d}. \tag{2}$$

Substituting Equation (2) (estimate $\mathbf{m}^{\text{est}}$) into Equation (1)**,** we obtain

$$\mathbf{d}^{\text{pre}} = \mathbf{G}\mathbf{m}^{\text{est}} = \mathbf{G}[\mathbf{H}\mathbf{d}^{\text{obs}}] = [\mathbf{G}\mathbf{H}]\mathbf{d}^{\text{obs}} = \mathbf{N}\mathbf{d}^{\text{obs}}. \tag{3}$$

Matrix $\mathbf{N} = \mathbf{G}\mathbf{H}$ is the m $\times$ m data resolution matrix (Wiggins, 1972). The data resolution matrix is only determined by the data kernel and the a priori information added to the problem. It is therefore independent of actual values of the data (Menke, 1984). Equation (3) shows the predicted values $\mathbf{d}^{\text{pre}}$ are weighting averages of the observed data $\mathbf{d}^{\text{obs}}$. The weighting function is the matrix $\mathbf{N}$. Each predicted datum is a weighted average of observed data with a row vector as a weighting function. For example, the ith estimated data $d_i^{pre} = \sum_{j=1}^{m} n_{ij} d_j^{obs}$, where n_{ij} is the jth element of the ith row of matrix $\mathbf{N}$ (Figure 1). If data have a natural ordering, a graph of elements of a row vector of $\mathbf{N}$ varying with column indices provides a sharpness of resolution (Figure 1). If the corresponding row vector is spike-like, the predicted data is well resolved. Otherwise, if

the corresponding row vector is broad, the predicted data is poorly resolved. The best scenario is **N** = **I** (**I** is the unit matrix), then each predicted value is uniquely determined.

The least-squares solution used in Xia et al.'s work (1999, 2002a, and 2003) would not possess the highest data resolution because the generalized inverse of the solution in the least-squares criterion is $\mathbf{H} = [\mathbf{G}^T\mathbf{G}]^{-1}\mathbf{G}^T$. The data resolution matrix **N** is

$$\mathbf{N} = \mathbf{GH} = \mathbf{G}[\mathbf{G}^T\mathbf{G}]^{-1}\mathbf{G}^T, \quad (4)$$

where **G** is the Jacobian matrix of the model with respect to S-wave velocity. Equation (4) shows data cannot be perfectly resolved in general because **N** is not the unit matrix. This is the result we normally obtained when applying an inverse algorithm that is based on a least-squares criterion. In the real world, however, Equation (4) provides a practical way to predict how well data can be resolved. The narrow peaks along the main diagonal of the matrix indicate that the data is well resolved. Data associated with larger diagonal values are those needed to define S-wave velocities for a given problem. Data associated with smaller diagonal values are those we do not have to have in defining S-wave velocities. In other words, if some necessary data (associated with higher diagonal values of the matrix **N**) are not available for a given problem, S-wave velocities cannot be estimated accurately.

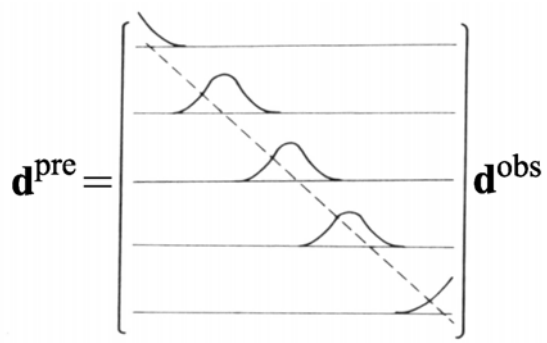

Figure 1. The data resolution matrix **N**. The narrow peaks along the main diagonal of the matrix indicate that the data is well resolved. (from Menke, 1984).

Examples of Data Resolution Matrix

The first model is a synthetic model from Xia et al. (1999). The model parameters are listed in Table 1. We calculated the data resolution matrix of the multi-layer model to show the different resolving power of each data and a different mode. We selected 31 data points at different frequencies up to the third mode. The row number of the matrix **N** associated with the data is listed in Table 2. If a frequency occurs more than once, the first occurrence is related to the fundamental mode, the second the second mode, and so on.

Table 1. An earth model parameters (Xia et al., 1999).

Layer number	$\mathbf{v}_s$ (m/s)	$\mathbf{v}_p$ (m/s)	ρ (g/cm^3)	**h** (m)
1	194.0	650.0	1.82	2.0
2	270.0	750.0	1.86	2.3
3	367.0	1400.0	1.91	2.5
4	485.0	1800.0	1.96	2.8
5	603.0	2150.0	2.02	3.2
The half space	740.0	2800.0	2.09	infinite

Table 2. Order of data points in the data resolution matrix of Model 1 (Table 1).

Row	1	2	3	4	5	6	7	8	9	10	11	12	13	14	15	16
Freq. (Hz)	2	3	5	10	15	20	25	25	30	30	35	35	35	40	40	40
Row	17	18	19	20	21	22	23	24	25	26	27	28	29	30	31	
Freq. (Hz)	45	45	45	50	50	50	55	55	55	60	60	60	70	70	70	

Figure 2 shows the data resolution matrix of the model shown in Table 1. We noticed that the diagonal elements generally possess highest values among elements of each row vector, which means predicted data are normally determined by measured data. We also noticed that elements 6 and 13 of the diagonal elements are among the largest values (Figure 3a), which means the fundamental phase velocity at 20 Hz and the third mode at 35 Hz are critical to define the S-wave velocities of the model (Table 1). The last nine data points including higher mode data, from 55 Hz to 70 Hz, are not necessary to define the model.

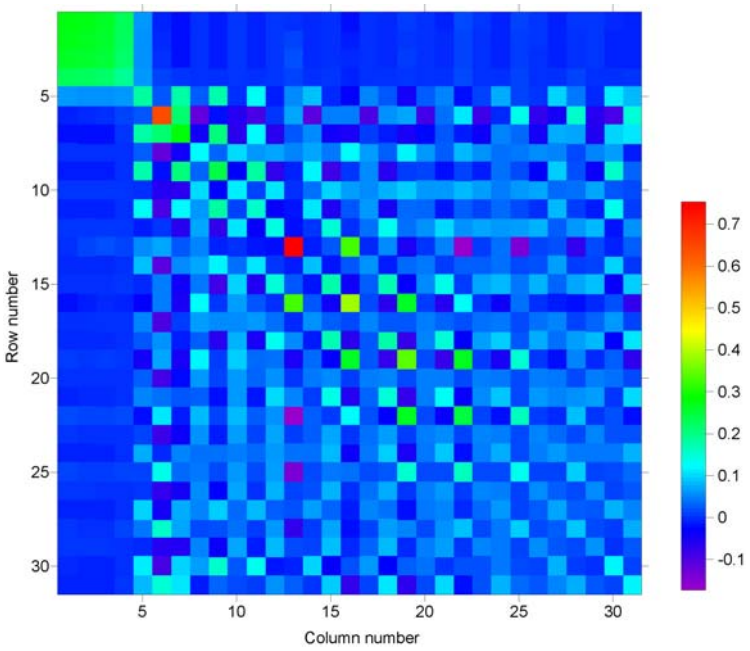

Figure 2. The data resolution matrix of the model shown in Table 1 (Xia et al., 1999).

With the data resolution matrix, we can explain why the higher mode data possess advantages in estimating S-wave velocities. We noticed that higher mode data possess higher diagonal values than do the fundamental data. Furthermore, the third mode data are resolved more easily than the second mode data (Figure 3a) because they possess higher values than the other modes. For example, the diagonal element of row 13 (the third mode data at 35 Hz) has value of around 0.8, which is much higher than the lower modes at the same frequency (rows 11 and 12). We plotted row vectors 12 and 13 in Figure 3b. Row vector 13 (the third mode data) is close to a spike function and centered at element 13, which indicated the data is well resolved. But row vector 12 (the second mode data) is very broad, which indicated the data is poorly resolved. In general, the third higher mode data (rows 13, 16, 19, 22, and 25) possess higher resolution values than the

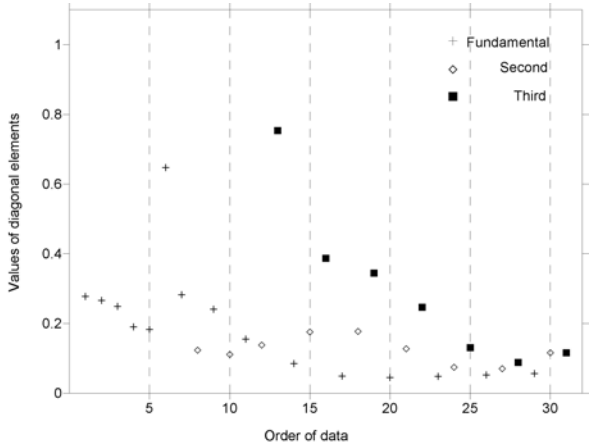

Figure 3a. Diagonal elements of the data resolution matrix in Figure 2.

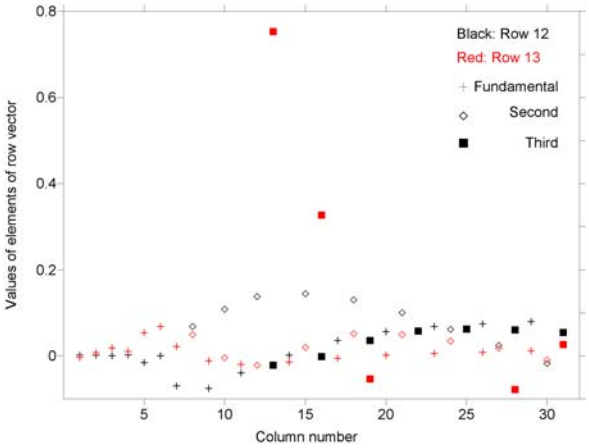

Figure 3b. Row vectors. Rows 12 and 13 of the data resolution matrix in Figure 2.

second higher mode data at the same frequencies (rows 12, 15, 18, 21, and 24). And the second mode data normally possess higher resolution values than the fundamental mode data at the same frequencies (rows 11, 14, 17, 20, and 23).

The second example is from Xia et al. (2003). The data were acquired in San Jose, California. The second mode data were well defined in the frequency-velocity domain (Xia et al., 2003). A 14-layer model with a layer thickness of 1 m was used to invert the Rayleigh-wave data. We calculated the data resolution matrix of the multi-layer model to show the different resolving power of each data and a different mode. We selected 35 data points at different frequencies up to the second mode. The row number of the matrix **N** associated with the data is listed in Table 3.

Table 3. Order of data points in the data resolution matrix of the San Jose example.

Row	1	2	3	4	5	6	7	8	9	10	11	12	13	14	15	16	17	
Freq. (Hz)	7	8	9	10	11	12	13	14	15	16	17	18	19	20	20	21	21	
Row	18	19	20	21	22	23	24	25	26	27	28	29	30	31	32	33	34	35
Freq. (Hz)	22	22	23	23	24	24	25	25	26	26	27	27	28	28	29	29	30	30

Figure 4 shows the data resolution matrix of the 14-layer model. As shown in Figure 2, the diagonal elements generally possess highest values among elements in each row vector, which means predicted data are normally determined by measured data. We noticed that the first 7 data from frequencies 7 to 13 Hz (rows 1 to 7) are critical to defining S-wave velocities. The second mode data at frequencies higher than 20 Hz (rows 15, 17, 19, 21, 23, 25, 27, 29, 31, 33, and 35) possess higher diagonal values than the fundamental mode data at the same frequencies (Figure 5a). For example, the fundamental mode data at frequency 21 Hz is poorly resolved due to its broad weighting function (Figure 5b), but the second mode data at the same frequency can be well resolved because of its spike-like weighting function (Figure 5b).

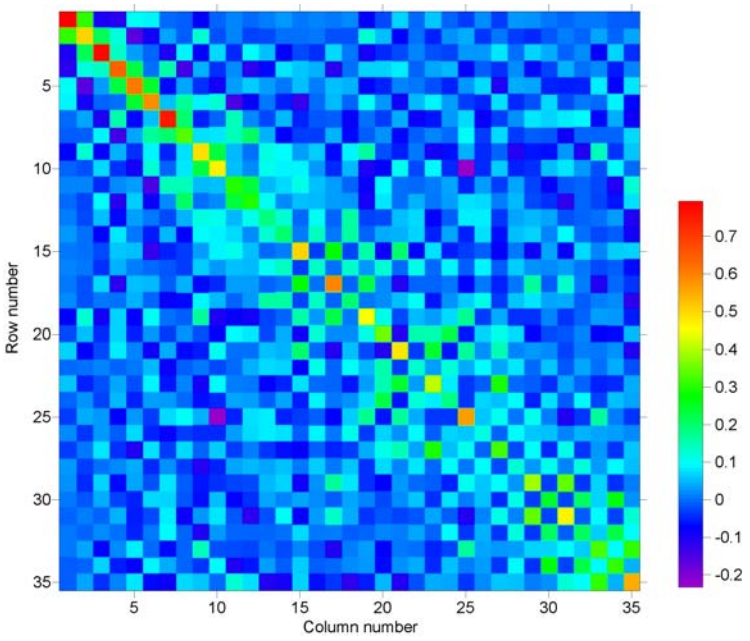

Figure 4. The data resolution matrix of the San Jose example (Xia et al., 2003).

The third example is also from Xia et al. (2003). These data were acquired in Vancouver, Canada. The second and third mode data were well defined in the frequency-velocity domain (Xia et al., 2003). A 14-layer model with a layer thickness of 2 m was used to invert the Rayleigh-wave data. We calculated the data resolution matrix of the multi-layer model to show the different resolving power of each data and a different mode. We selected 35 data points at

different frequencies up to the second mode. The row number of the matrix **N** associated with the data is listed in Table 4.

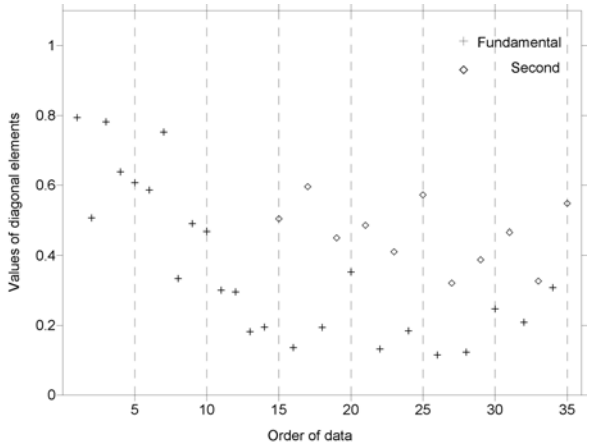

Figure 5a. Diagonal elements of the data resolution matrix in Figure 4.

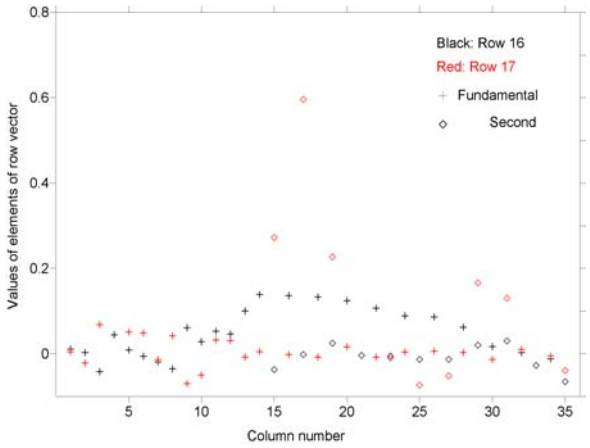

Figure 5b. Row vectors. Rows 16 and 17 of the data resolution matrix in Figure 4.

Table 4. Order of data points in the data resolution matrix of the Vancouver example.

Row	1	2	3	4	5	6	7	8	9	10	11	12	13	14	15	16	17	
Freq. (Hz)	7	9	11	13	15	17	17	19	19	21	21	23	23	23	25	25	25	
Row	18	19	20	21	22	23	24	25	26	27	28	29	30	31	32	33	34	35
Freq. (Hz)	27	27	27	29	29	29	31	31	31	33	33	33	35	35	35	37	37	37

Figure 6 shows the data resolution matrix of the 14-layer model. As discussed previously, the diagonal elements generally possess highest values among elements of each row vector, which means predicted data are normally determined by measured data. We noticed that the fundamental data at frequencies 7 and 9 Hz and the second higher mode data at 17, 19, 21, 23, 25, 28, 31, 33, 35, and 37 Hz are crucial in defining the S-wave velocity model for given geological problem. It is interesting to note that the third mode data for this model do not show higher resolving power than the second mode data (Figure 7a). For this particular model, data at frequencies from 7 to 9 Hz are resolved exactly. These data are extremely important in the inversion. For comparison, we plotted row vectors 6 and 7, which are the fundamental mode and the second mode at frequency 17 Hz

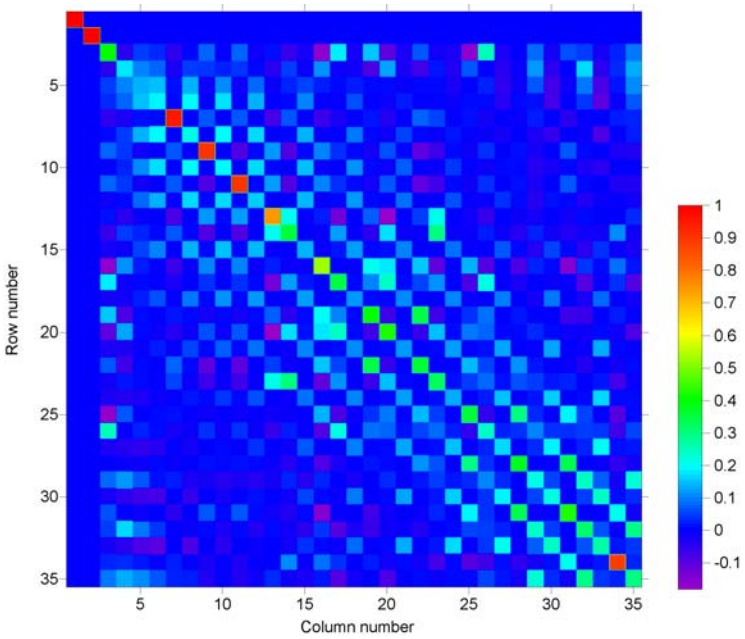

Figure 6. The data resolution matrix of the Vancouver example (Xia et al., 2003).

(Figure 7b). Clearly, the fundamental data (row 6) is poorly resolved because of its broad weighting function and the second mode data at the same frequency (row 7) is well resolved due to its spike-like weighting function.

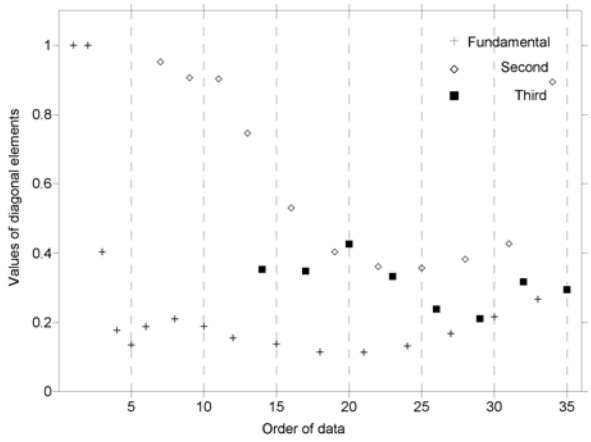

Figure 7a. Diagonal elements of the data resolution matrix in Figure 6.

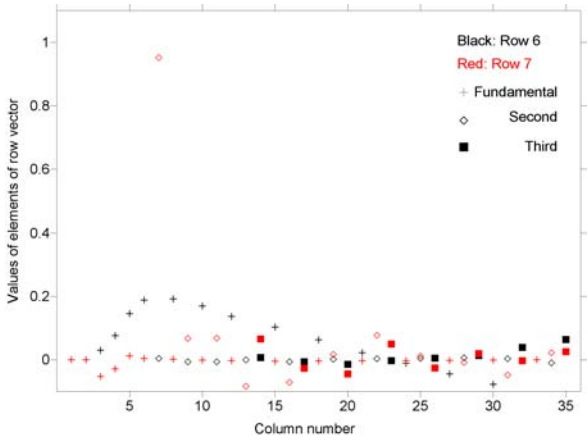

Figure 7b. Row vectors. Rows 6 and 7 of the data resolution matrix in Figure 6.

Practical Implication of the Data Resolution Matrix

Data resolution matrices in the previous section showed that higher mode data generally are well resolved for the given models. In practice, we only know an initial model for a given problem. Is it possible to select data based on the data resolution matrix of an initial model? We mentioned in the previous section that some data are well resolved because of the higher values of the diagonal elements. Is it feasible to use only these data that possess higher values of the diagonal elements in the inversion to obtain accurate S-wave velocity model? We address these questions below.

We used the model showed in Table 1. Suppose S-wave velocities for all layers are 25% lower than the true model (Table 1), which are 146, 202, 275, 363, 452, and 555 m/s, respectively, we recalculated the data resolution matrix and showed its diagonal elements in Figure 8a. We also suppose S-wave velocities for all layers are 25% higher than the true model, which are 242, 337, 458, 606, 753, and 925 m/s, respectively. We recalculated the data resolution matrix and showed those diagonal elements in Figure 8b.

The similarity between Figure 3a and Figure 8 is obvious. First, higher mode data possess higher values along diagonal elements than do lower mode data. Second, the frequency ranges of data with higher values along diagonal elements are pretty much the same, which suggested that it is possible to select data based on the data resolution matrix of an initial model. For example, if we set a threshold of 0.175, which means that only data with a diagonal value higher than 0.175 will based in the inversion. The selections from Figure 3a and Figure 8a are very close. Except for the data at the higher frequencies, the selection from Figure 8b, where velocities are 25% higher than true model, are also close to the selection from Figure 3a.

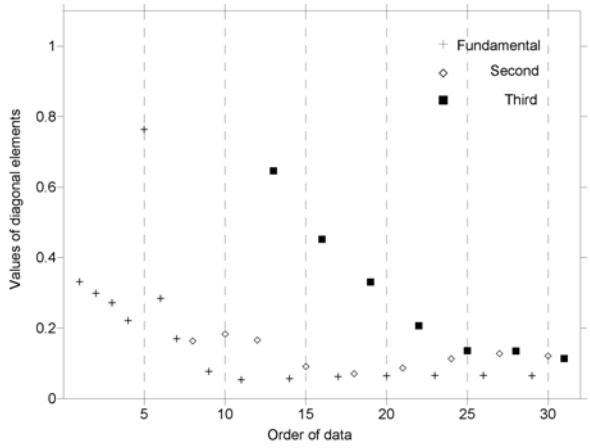

Figure 8a. Diagonal elements of the data resolution matrix of the model showed in Table 1 except S-wave velocities are 25% lower than those showed in Table 1.

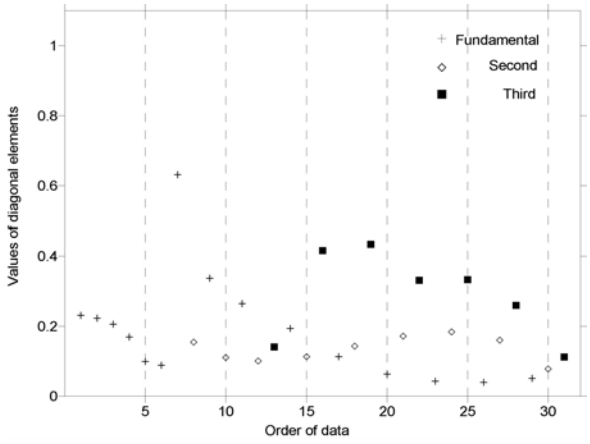

Figure 8b. Diagonal elements of the data resolution matrix of the model showed in Table 1 except S-wave velocities are 25% higher than those showed in Table 1.

To answer the second question, let us look at the synthetic example first. We selected 14 data from Figure 3a that possess the diagonal values of 0.175 and higher (Table 5 in red) to perform an inversion. The initial model was the same used in Xia et al. (1999). We listed inverted results and results from Xia et al. (1999) in Table 6 with the true and initial models. Results from Xia et al. (1999) only used the fundamental mode data. Although calculated phase velocities from both models fit data with the root-mean-square error less than 2 m/s, the model obtained from the data in red in Table 5 is much better than the model obtained using only the fundamental data (Xia et al., 1999). Notice that we only used 14 phase velocities in inversion to obtain the almost perfect inverted model. The model obtained using only the fundamental data (45 phase velocities) cannot distinguish layers 4 and 5 because the data (points 14, 17, 20 in Figure 3a) affected most by these layers are poorly resolved.

Table 5. Data selected in inversion in red (Model from Xia et al., 1999).

Row	1	2	3	4	5	6	7	8	9	10	11	12	13	14	15	16
Freq. (Hz)	2	3	5	10	15	20	25	25	30	30	35	35	35	40	40	40
Row	17	18	19	20	21	22	23	24	25	26	27	28	29	30	31	
Freq. (Hz)	45	45	45	50	50	50	55	55	55	60	60	60	70	70	70	

Table 6. Inversion results. The unit is in m/s.

True	Initial	Inverted with data listed in Table 5 in red	Inverted (Xia et al., 1999)
194	230	194	194
270	272	270	272
367	330	367	351
485	397	486	539
603	453	600	535
740	1036	740	741

We selected 16 data from Figure 5a that possess diagonal values of 0.450 and higher (Table 7 in red) to perform inversion. Sixteen data points are almost the minimum number of data needed to solve the problem with 14 unknowns. The initial model was the same used in Xia et al. (2003). We showed inverted results and inverted results from multi-mode data (Xia et al., 2003) in Figure 9 with the best-inverted model that was obtained from "error-free" data (we listed this model as "true" in Figure 9). Overall, inversion results of the selected data are closer to the "true" model than results from multi-mode data (Xia et al., 2003).

Table 7. Data selected in inversion in red (the San Jose example, Xia et al., 2003).

Row	1	2	3	4	5	6	7	8	9	10	11	12	13	14	15	16	17	
Freq. (Hz)	7	8	9	10	11	12	13	14	15	16	17	18	19	20	20	21	21	
Row	18	19	20	21	22	23	24	25	26	27	28	29	30	31	32	33	34	35
Freq. (Hz)	22	22	23	23	24	24	25	25	26	26	27	27	28	28	29	29	30	30

We selected 14 data from Figure 7a (the fundamental data from 7 to 11 Hz at a 1 Hz interval and the second mode data from 17 to 25 Hz at a 1 Hz interval) that possess diagonal values of 0.40 and higher from 7 to 25 Hz, the same range used by Xia et al. (2003), to perform this inversion. The initial model was the same used in Xia et al. (2003). We showed inverted results and inverted results from multi-mode data (Xia et al., 2003) in Figure 10 with the borehole measurements. Inversion results of the selected data are closer to the "true" model than results from multi-mode data up to 15-m in depth than results from multi-mode data. For the deeper part (> 15 m), Figure 10 showed a significant deviation of inverted results from borehole measurements. No improvement could be made for this part of the model because the longest wavelength of the fundamental mode (the second mode) data is around 23 m (11 m). With these data, as indicated in Xia et al. (2003), the maximum depth of investigation is around 15 m.

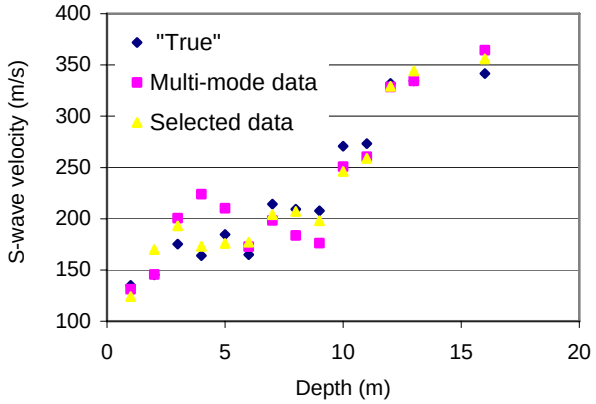

Figure 9. Inversion results of the San Jose example. Model "Selected data" was the inverted model from data selected based on data resolution functions.

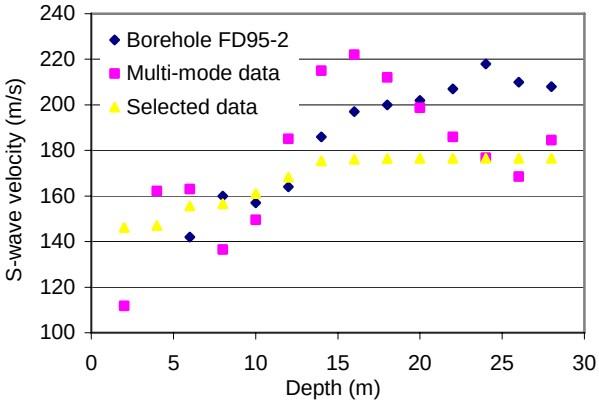

Figure 10. Inversion results of the Vancouver example. Model "Selected data" was the inverted model from data selected based on data resolution functions.

Conclusions

We used the data resolution matrix to show that higher mode data possess higher data resolution power than the lower mode data, in general. This property explains why inversion of

higher mode data normally provides more accurate results. Examples showed that the inverted models from data selected based on data resolution functions are better than models inverted from multi-mode data that were not selected. A threshold for data selection varies with the data resolution matrix of a geophysical model. But the number of data selected should be larger than the number of layers in an S-wave velocity model. Because the data resolution matrix is only related to the data kernel and a priori information applied to the problem not the function of data (Menke, 1984), we can use the data resolution matrix to set requirements of data for a given problem, such as data existence in a specific frequency range. In some cases, we may have to modify the investigation depth and the thickness of layers based on the data resolution matrix. As the Vancouver example indicated, the investigation depth should be shallower than 26 m or data with longer wavelength should be acquired to estimate S-wave velocities for the 26-m thick model.

References

Aki, K., and Richards, P.G., 1980, Quantitative seismology: W.H. Freeman and Company, San Francisco.

Beaty, K.S., and Schmitt, D.R., 2003, Repeatability of multimode Rayleigh-wave dispersion studies, Geophysics, 68(3), 782-790.

Beaty, K.S., Schmitt, D.R., and Sacchi, M., 2002, Simulated annealing inversion of multimode Rayleigh wave dispersion curves for geological structure: Geophys. J. Int., 151**,** 622–631.

Dorman, J., and Ewing, M., 1962, Numerical inversion of seismic surface wave dispersion data and Crust-Mantle structure in the New York-Pennsylvania area: J. Geophys. Res., 67, 5227-5241.

Liang, Q., and Chen, C., in review, Rayleigh wave inversion limitations from selecting multimode dispersion data: Near Surface Geophysics.

Luo, Y., Xia, J., Liu, J., Liu, Q., and Xu, S., in review, Joint inversion of high-frequency surface waves with fundamental and higher modes: Journal of Applied Geophysics.

Menke, W., 1984, Geophysical data analysis—Discrete inversion theory: Academic Press, Inc., New York.

Park, C.B., Miller, R.D., and Xia, J., 1999, Multi-channel analysis of surface waves: Geophysics, 64(3), 800-808.

Rix, G.J., Lai, C.D., and Spang Jr., A.W., 2000, In situ measurement of damping ratio using surface waves: Journal of Geotechnical and Geoenvironmental Engineering, 126(5), 472-480.

Song, Y.Y., Castagna, J.P., Black, R.A., and Knapp, R.W., 1989, Sensitivity of near-surface shear-wave velocity determination from Rayleigh and Love waves: Technical Program with Biographies, SEG, 59th Annual Meeting, Dallas, Texas, 509-512.

Song, X., Gu, H., Liu, J., and Zhang, X, in press, Estimation of shallow subsurface shear-wave velocity by inverting fundamental and higher-mode Rayleigh waves: Soil Dynamics and Earthquake Engineering.

Stokoe, K.H., II, and Nazarian, S., 1983, Effectiveness of ground improvement from spectral analysis of surface waves: Proceeding of the Eighth European Conference on Soil Mechanics and Foundation Engineering, Helsinki, Finland.

Stokoe, K.H., II, Rix, G.J., and Nazarian, S., 1989, In situ seismic testing with surface wave: Processing, XII International Conference on Soil Mechanics and Foundation Engineering, 331-334.

Wiggins, R.A., 1972, The general linear inverse problem: Implication of surface waves and free oscillations for Earth structure: Rev. Geophys. Space Phys., 10, 251-285.

Xia, J., Miller, R.D., and Park, C.B., 1999, Estimation of near-surface shear-wave velocity by inversion of Rayleigh wave: Geophysics, 64(3), 691-700.

Xia, J., Miller, R.D., Park, C.B., Hunter, J.A., and Harris, J.B., 2000a, Comparing shear-wave velocity profiles from MASW with borehole measurements in unconsolidated sediments, Fraser River Delta, B.C., Canada: Journal of Environmental and Engineering Geophysics, 5(3), 1-13.

Xia, J., Miller, R.D., and Park, C.B., 2000b, Advantage of calculating shear-wave velocity from surface waves with higher modes: Technical Program with Biographies, SEG, 70th Annual Meeting, Calgary, Canada, 1295-1298.

Xia, J., Miller, R.D., Park, C.B., Hunter, J.A., Harris, J.B., and Ivanov, J., 2002a, Comparing shear-wave velocity profiles from multichannel analysis of surface wave with borehole measurements: Soil Dynamics and Earthquake Engineering, 22(3), 181-190.

Xia, J., Miller, R.D., Park, C.B., and Tian, G., 2002b, Determining Q of near-surface materials from Rayleigh waves: Journal of Applied Geophysics, 51(2-4), 121-129.

Xia, J., Miller, R.D., Park, C.B., and Tian, G., 2003, Inversion of high frequency surface waves with fundamental and higher modes: Journal of Applied Geophysics, 52(1), 45-57.

Xia, J., Xu, Y., Miller, R.D., and Chen, C., 2006, Estimation of elastic moduli in a compressible Gibson half-space by inverting Rayleigh wave phase velocity: Surveys in Geophysics. 27(1), 1-17.